
CFD simulations of Flow Field in Flapper-Nozzle Pilot Valve with Vortex Generators

Tong Li

dept. of fluid control and automation

Harbin Institute of Technology

Harbin, China

18b908121@stu.hit.edu.cn

Jinghui Peng*

dept. of fluid control and automation

Harbin Institute of Technology

Harbin, China

jpeng@hit.edu.cn

Songjing Li*

dept. of fluid control and automation

Harbin Institute of Technology

Harbin, China

lisongjing@hit.edu.cn

Abstract.

For the flapper-nozzle servo valve, the existence of the flow separation phenomenon in the pilot stage may lead to self-excited oscillation, which is a hidden danger to the stability of the servo valve. Aiming at improving the flow state and the stability of the flow field in the pilot stage, a new structure of flapper with vortex generators without disturbing the control performance of the pilot stage is designed. The flow separation phenomenon in the pilot stage is confirmed by analyzing the flow with traditional flapper under different inlet pressures. The flow field in the pilot stage is explored using vortex generators compared to traditional one, the results show that the flow state of the pilot stage flow field is changed by the novel flapper with vortex generators, the flow separation phenomenon is well controlled, the number of vortices in the flow field is significantly reduced, and the flow field is more stable. Therefore, the compact and effective vortex generators have a good effect on improving the stability of the flow field in the pilot stage of flapper-nozzle servo-valve. The primary parameters of vortex generators, height and location, are also taken into account, it is found that when the height of vortex generators $h=0.2$ and the location size $l=0.4$, it is more suitable for the actual situation.

Keywords. Flapper-nozzle pilot valve; flow field; flow separation; vortex generators

1. INTRODUCTION

Electro-hydraulic servo technology is an important drive and transmission technology widely used in aerospace, national defense and modern production fields. As an indispensable core component of electro-hydraulic servo system, the stability of servo valve has a vital influence on the reliable operation of the whole servo system. Many studies show that the stability of servo valve is closely related to the flow field of the pilot stage.

The pilot stage flow field refers to the area formed by nozzle, flapper and fixtures, the jet from the nozzle impinging on the flapper and then flows to the outlet. Different from the ordinary impingement jet, the flapper in the pilot stage is neither a flat plate nor a cylinder,

but a combination of cylinder and plane. However, to the best of the author's knowledge, few attentions are paid to this type of impingement jet. Experimental and numerical investigations of cavitation phenomenon appearing in the flow field between the flapper and nozzle of an electrohydraulic servo-valve are carried out in [1], one of their discoveries is that at lower Reynolds numbers, such as $Re=630$ and $Re=1060$, the flow moves around the flapper, however, with the increase of Reynolds number, the flow gradually separates from the flapper surface, and cavitation is more obvious. Cavitation phenomenon causes pressure pulsation in flow field and increases the possibility of self-excited oscillation. Furthermore, according to [2], separation of flow and a relative motion between solids contacting in liquid are two possible ways for cavitation. The flow separation is the reason of the large-amplitude oscillation of the flow fields around the inverted flag as in [3], Therefore, it is necessary to research the method of controlling flow separation.

Flow separation phenomenon is very common, such as cylinder flow and aircraft stall phenomenon. The vortex generator (VG), as one of the most successful designs in aviation history, has been highly regarded since its invention in the 1940s and has been applied in many fields. In order to improve the aerodynamic performance of tilt-rotor aircraft, the flow characteristics of V-22 airfoil without and with two rows of parallel vortex generators are studied by numerical simulation [4]. The role of vortex generator in controlling and suppressing dynamic stall on a wind turbine airfoil under unsteady conditions is studied in [5]. Aiming at the problem of excessive propeller excitation force and hull vibration noise of a ship, a triangular vortex generator is designed and installed on the surface of ship stern [6]. The counter-rotating streamwise vortices induced by micro-VGs had a rectifying effect on the near-wall flow and withstood the flow disturbance in the spanwise direction [7].

From the above research, it can be seen that the vortex generator has a good role in delaying flow separation. Therefore, based on the special flow field structure and the flow state of flapper-nozzle pilot stage, a new flapper with vortex generators arranged in pairs at certain angles on its surface is proposed.

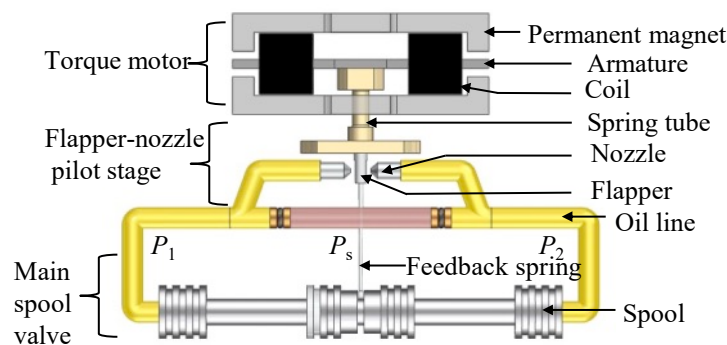


Figure 1.1. Structure of flapper-nozzle servo-valve

2. THE STRUCTURE OF FLAPPER-NOZZLE SERVO-VALVE

Double flapper-nozzle servo-valve is one of the most widely used servo-valve structures. Figure 1.1 is the structure schematic diagram of the servo-valve in the null position. The servo-valve is mainly composed of two parts, electromagnetic part and hydraulic part. The

electromagnetic part, also known as torque motor, including permanent magnet, armature, coil, etc. The role of torque motor is to convert the control signal into mechanical movement. The hydraulic part includes a flapper-nozzle pilot stage and a power stage of spool valve. The pilot stage includes nozzle, flapper, spring tube, feedback spring, etc., and the power stage is mainly composed of spool and valve sleeve. The combination of armature, flapper, spring tube and feedback spring is called armature component.

3. FLOW FIELD OF THE PILOT STAGE

The flow field of the pilot stage is the area surrounded by nozzle, flapper and wall. When the servo valve is in operation, the high-pressure oil is emitted from the nozzle, after a short distance of free jet flow, it impinges on the flapper and then flows in all directions with the stagnation point as center, at this point, the flow state is equivalent to wall jet flow, a small part of the fluid flows to the outlet along the flapper plane, and at the same time, most of the fluid flows away from the flapper to the housing wall, and then reverse. The fluid is separated when it impacts the housing wall and flows in the reverse direction, part of the fluid is affected by the incoming flow, the housing wall and the nozzle wall and rotates in the counterclockwise direction, the other part of the fluid flows under the constraint of the cylindrical wall and then couplings with the fluid emitted from the opposite nozzle, under the influence of the flapper wall, a vortex is formed. Flow separation occurs approximately after the fluid leaves the flapper.

4. VORTEX GENERATOR

The basic principle of vortex generator to control flow separation is to generate streamwise vortices with high energy. Such streamwise vortices are mixed with the downstream low-energy boundary layer flows, and the energy is transferred to the boundary layer, so that the boundary layer flow field in adverse pressure gradient can continue to attach to the body surface without separation after obtaining additional energy, as see in Figure 4.1.

In order to control the flow separation phenomenon, the vortex generator is adopted in this paper. Shape, size and installation position are three key parameters of vortex generator design. In terms of shape, the geometric shape of vortex generator includes airfoil, rectangular plate, triangular plate and dipole surface [6]. Combined with the installation space and the effect of delaying separation, the triangular vane vortex generator is selected in this paper, and the size of the vortex generator is set according to [8]. The installation form and specific size are shown in Figure 4.2(a). Vortex generator arrangement is determined based on five parameters: height h , length m , pair distance n , local flow incidence angle β and distance l relative to the center line of the nozzle, as shown in Figure 4.2(b). Relevant research shows that the height and installation position of vortex generator are particularly important among vortex generator parameters [5,8,9]. Therefore, the height and installation position of vortex generator are studied in this paper.

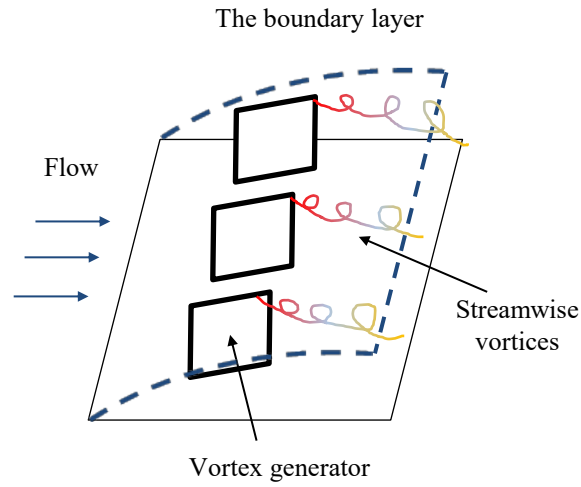


Figure 4.1. Vortex generator

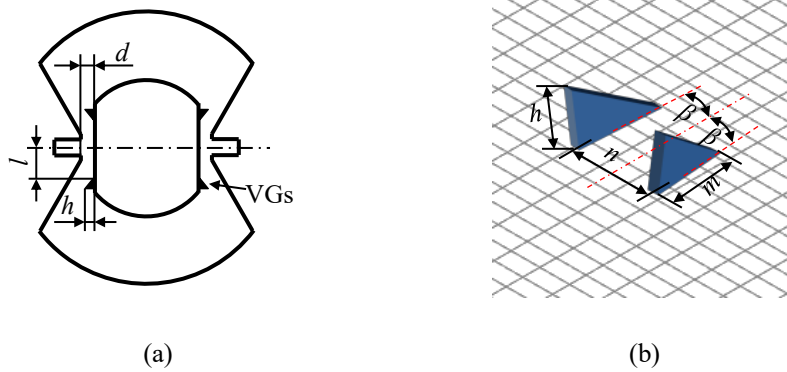


Figure 4.2. Structure of vortex generator: a. Schematic diagram of installation position of vortex generators; b. Triangular vane type vortex generator.

4.1. Determination of vortex generator height h

Vortex generators transfers momentum from the external flow to the near wall region, so that the flow is well attached to the wall. Therefore, the height of vortex generators is usually related to the local boundary layer thickness [4]. The boundary layer thickness of impinging jet on smooth surface and low Reynolds number is as follows [10]:

$$\frac{z(u_{\max})}{D} = \frac{3.2}{\sqrt{Re_1}} \sqrt{\frac{rW_{\text{jet}}}{Du_{\max}}} \quad \text{for } Re_1 < 2.5 \times 10^4 \quad (4.1)$$

where $z(u_{\max})$ is the distance from plate corresponding to maximum radial mean velocity, m; D is diameter of the jet pipe, m; Re_1 is local Reynolds number, r is the radius from the stagnation point, m; W_{jet} is axial jet velocity at the center of the pipe outlet, m/s; u_{\max} is the maximum radial mean velocity for a specified r , m/s.

$$Re_1 = ru_{\max} / \nu \quad (4.2)$$

where ν is the kinematical viscosity, m^2/s .

It is estimated that when the inlet pressure is 4MPa, the local boundary layer thickness ($z(u_{\max})$) at $r=0.3$ is $1.8 \times 10^{-5}m$. For nozzle-flapper pilot stage, the size of vortex generator is affected by various factors, flow field space ($d \approx 2 \times 10^{-4}m$), manufacturing feasibility, and boundary layer thickness. From this, the influence of different vortex generator heights ($h=0.05, 0.1, 0.2mm$) on the delay of flow separation is investigated in this paper.

4.2. Determination of other shape parameters of vortex generator

The installation form of vortex generators are shown in Figure 4.2. As only the vortex generator is added to the flapper, other dimensions are the same as before. The diameter of the flapper is 2mm, and the width of the flapper plane is about 1.32mm. In addition, to prevent impact on the impingement jet, the vortex generators should be arranged outside the projection area of the nozzle on the flapper plane, so the installation position of the vortex generator should meet the following relationship.

$$l > D/2 \quad (4.3)$$

$$l + m < 1.32/2 = 0.66mm \quad (4.4)$$

In this paper, the length of vortex generator m is set to 0.15mm, and the diameter of the nozzle D is 0.3mm, Therefore, the range of installation position parameter l of vortex generator is 0.15 ~ 0.51mm, and $l = 0.3, 0.4$ and 0.5 are selected to study the influence of the installation position of vortex generators on delaying flow separation. The vane thickness is set to the ideal state, which is 0.01mm. The pair distance n is set to 0.1mm, and the local flow incidence angle β is 15° .

5. IMPLEMENTATION OF NUMERICAL STUDY

5.1. Geometry model and computational domain of pilot stage

The overall size of the flow field of the pilot stage is small and the experiment is complicated, it will cost a lot of time and money to conduct experimental research on the influence of all different parameters on the flow field. Therefore, simulation research is necessary, and which is performed with Star-ccm+ software.

5.2. Meshing and boundary conditions

The structure of the whole model is symmetrical, in order to save computing resources and time, half of the model is used for simulation. The turbulence model and the detailed parameters are set according to the previous work [1]. Star-ccm+ software is used to complete the mesh division of the model, and the overall mesh size is 0.1mm. Since the vortex generator structure is mainly used to generate vortices in the boundary layer, this paper considers the influence of boundary layer and refines the boundary layer near the flapper wall. The thickness of boundary layer is set to 33% of the basic grid size, i.e. 0.03mm, the number of inner boundary layer is set to 10, and the growth rate of boundary layer is set to 1.5. In addition, the grid size in the boundary layer is set to 0.025mm. Boundary conditions are also considered, the two inlet types are set as stagnation inlet with pressure of 2,4,6,8Mpa, respectively; and the two outlet types are pressure outlet with pressure of 0MPa; the middle

surface ($x=0$) type is set as symmetry plane; the other surfaces are wall, as shown in Figure 5.1. In addition, the viscosity of oil is 0.0085kg/ms , the density of oil is 850kg/m^3 .

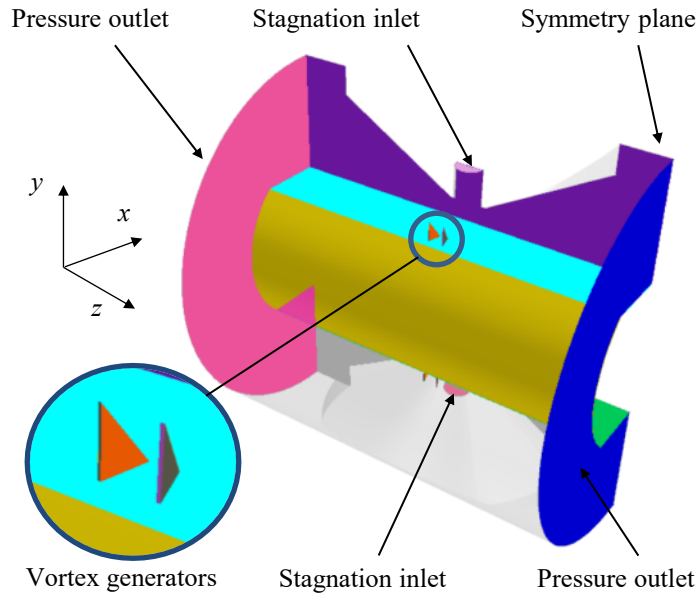


Figure 5.1. 3D model and boundary type setting

6. RESULTS AND DISCUSSION

6.1. Flow field under different inlet pressures

Figure 6.1 shows the velocity scalar diagram of the flow field in the pilot stage under different inlet pressures. As can be seen from the figure, when the inlet pressure p_i is 2MPa, the pressure energy is small, the kinetic energy of jet is relatively small, and the liquid flow velocity is small, the maximum velocity is 66.8m/s. After leaving the flapper plane, the liquid flow along the cylinder wall of the flapper, which is consistent with the Coanda Effect. With the increase of inlet pressure, when p_i is 4MPa, the pressure energy, kinetic energy and flow velocity increase, and the maximum velocity is 94.4m/s, after leaving the flapper plane, most of the fluid still flows along the cylinder wall of the flapper, and a small part of the liquid flows away from the flapper wall, resulting in flow separation. When p_i is 6MPa, the maximum velocity reaches 116m/s, most of the liquid continues to flow along the original flow direction after leaving the flapper plane, and a small part flows along the cylinder wall. When p_i is 8MPa, the maximum velocity reaches 134m/s, the flow field is roughly divided into four parts, and the flow separation phenomenon is more obvious. This is consistent with previous research [1].

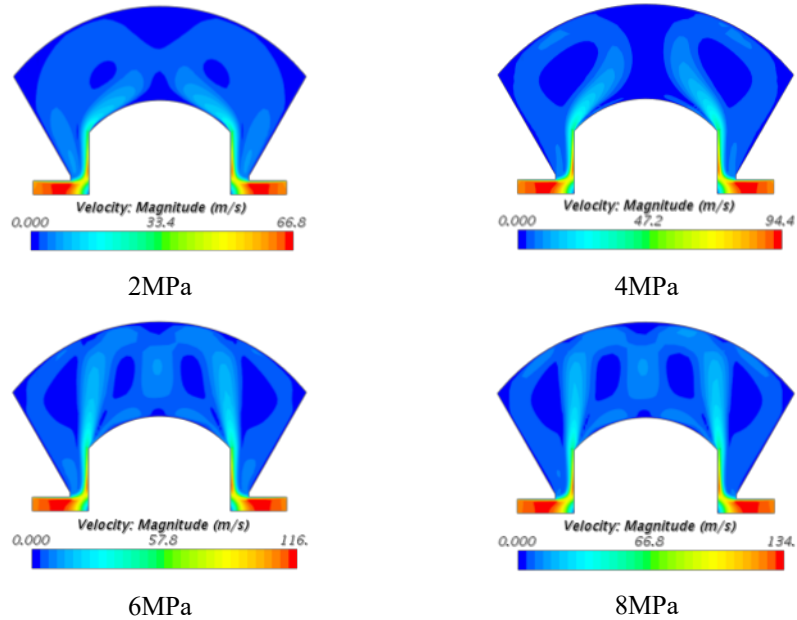


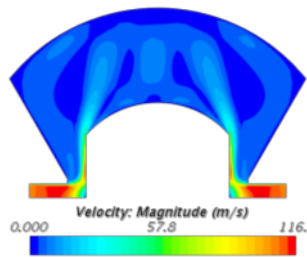
Figure 6.1. Velocity scalar diagram of pilot stage flow field under different inlet pressures based on conventional flapper

6.2. Flow separation delay

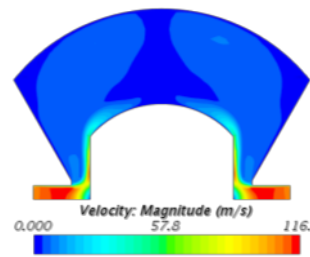
For the sake of suppress the flow separation phenomenon, the vortex generators are introduced in this paper, and the effect of the vortex generators are studied.

Figure 6.2 shows the flow state comparison diagram of flow field in the pilot stage with vortex generators and smooth. The inlet pressure p_i of both is 6MPa, and the parameters of the vortex generators are $h=0.2$ and $l=0.4$. Figure 6.2(a) and (b) are velocity scalar diagrams of flow field with vortex generators and smooth respectively. As can be seen from the figure, when the vortex generators are installed on the flapper plate, the oil flow still flows along the flapper surface after passing through the junction of plane and camber of the flapper, and the flow state is more stable than that without vortex generators.

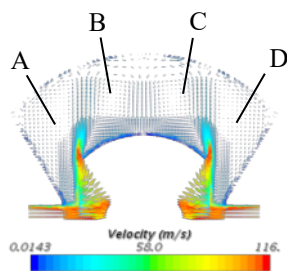
Figure 6.2(c) and (d) are velocity vector diagrams of flow field with vortex generators and smooth respectively. It can be seen more clearly from the vector figure that when there are no vortex generators, the oil flow is separated at the junction of plane and camber of the flapper, thus four vortices are formed in the flow field, in which A and C are counterclockwise, B and D are clockwise, and the four vortices almost occupy the whole flow field. However, in the flow field with vortex generators installed, the liquid flow continues to flow along the flapper camber, and only two small vortices are formed in the flow field, E in the counterclockwise direction and F in the clockwise direction. The flow field is relatively more stable.



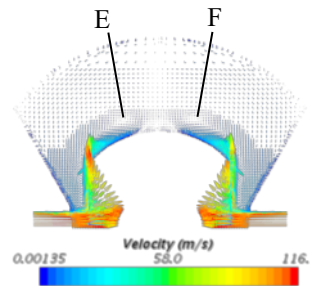
(a) smooth



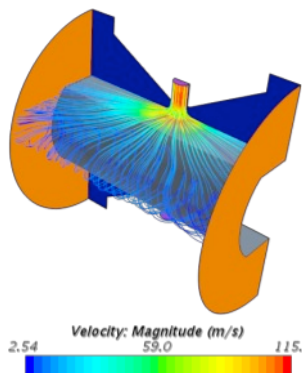
(b) with VGs



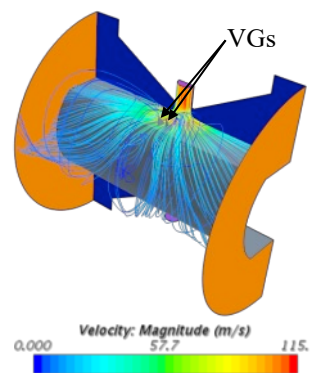
(c) smooth



(d) with VGs



(e) smooth



(f) with VGs

Figure 6.2. Comparison of flow state with or without vortex generators
 Figure 6.2 (e) and (f) is the 3d flow diagram of the flow field, from which the flow state of the fluid can be clearly seen. As can be seen from Figure 6.2(e), the fluid continues to flow in the original direction after breaking away from the flapper plane, and after hitting the housing wall, it reenters and forms a counterclockwise vortex coupled with the flow from the other inlet. While in Figure 6.2(f), with the presence of vortex generators, the fluid continues to flow close to the cylinder wall of the flapper after leaving the flapper plane and forms a clockwise vortex coupled with the flow from the other inlet.

6.3. Pressure distribution and vortices

Figure 6.3 shows pressure and vorticity field of flow field with vortex generators and smooth. The pressure is still 6MPa, and the parameters of the vortex generator are $h=0.2$, $l=0.4$. As can be seen from Figure 6.3(a) and (b), a low pressure area appears behind the junction of flapper plane and camber in the flow field with or without vortex generator, A1 in Figure 6.3(a) and A2 in Figure 6.3(b), which are equivalent to wakes in the flow field. A low pressure area also appears at B in Figure 6.3(b) due to the presence of the vortex generators. In addition, it can be seen from Figure 6.3(a) that there are four large low-pressure areas in the flow field, which are formed by vortices in the flow field, corresponding to Figure 6.2(c). The two areas with low relative pressure in Figure 6.3(b) correspond to Figure 6.2(d), which is also caused by vortices in the flow field. Figure 6.3(c) and (d) are vorticity fields. The vortices in Figure 6.3(c) correspond to Figure 6.2(c) and Figure 6.3(a). Flow separation generates vortices and the formation of vortices generates a low pressure area. In the flow field with vortex generators, the flow separation phenomenon is suppressed, the number of vortices is reduced, and the flow field is more stable, as shown in Figure 6.3(d).

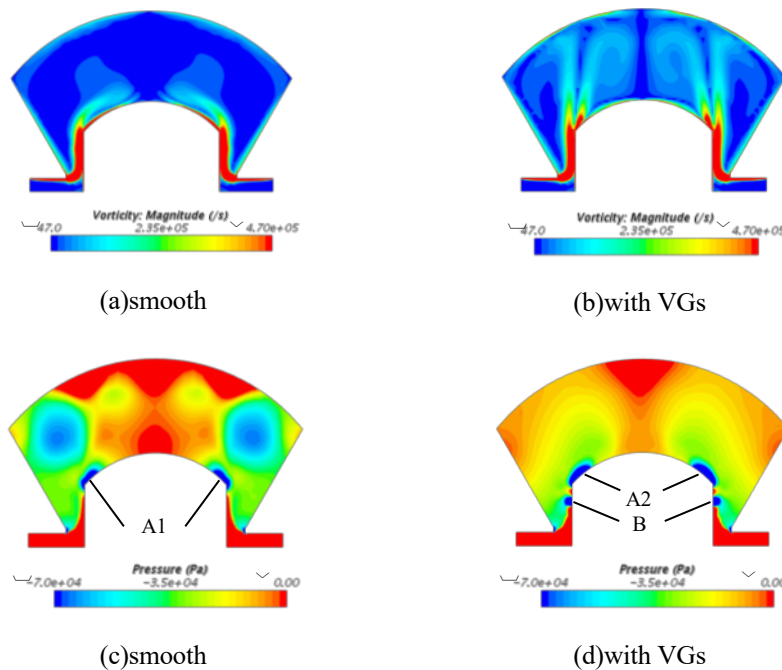


Figure 6.3. Pressure field and vorticity field

6.4. Effect of vortex generator dimension

The instability in the flow field of the pilot stage is mainly caused by the turbulent flow, so the turbulent kinetic energy is selected in this paper to represent the influence of the vortex generators parameters on the flow field. In order to fully express the flow field, six points are taken as detection points in the flow field to study the stability of the flow field, as shown in Figure 6.4. And the coordinates of the detection points are shown in Table 6.1.

The influence of the height and location of the key geometric parameters on the effect of the vortex generator is simulated. The inlet pressure is set as 6MPa, and the $l=0.4$ is selected for the position of vortex generators. The average value of turbulent kinetic energy within 0.01s after the flow field is stabilized is taken as the data point to plot. Figure 6.5. shows the turbulent kinetic energy of flow field with different vortex generators height ($h=0.05, 0.1, 0.15, 0.2$). As can be seen from the figure, compared with the traditional flapper, the turbulent kinetic energy of the flow field with vortex generators at points P2 and P5 decreases substantially by about 80%. Meanwhile, the turbulent kinetic energy at points P1, P3, P4 and P6 does not change much, so the vortex generators play a role in improving the stability of the flow field in the pilot stage. In the flow field with vortex generators, the overall turbulent kinetic energy of the flow field decreases with the increase of the height of the vortex generators, and the flow field is relatively more stable. If the height of vortex generators is too small, it is difficult to be machined; if the height is too large, it may interfere with the wall and cannot be assembled. Therefore, $h=0.2$ is relatively appropriate.

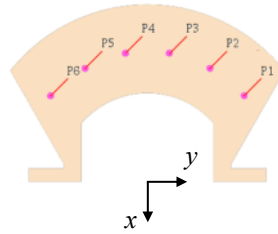


Figure 6.4. Detection points

Table 6.1. The coordinates of the detection points

coordinates	P1	P2	P3	P4	P5	P6
$x(\text{mm})$	-0.97	-1.28	-1.45	-1.45	-1.28	-0.97
$y(\text{mm})$	1.1	0.71	0.25	-0.25	-0.71	-1.1
$z(\text{mm})$	0	0	0	0	0	0

In order to study the influence of vortex generator location on the flow field, the inlet pressure p_i is still set as 6MPa. If the height h of the vortex generator is too large, the height of the vortex generator is the main influence, which is not conducive to analyzing the influence of the vortex generator location on delaying flow separation, therefore, the height h is selected as 0.05 here. The location parameters of vortex generators are $l=0.3, 0.4$ and 0.5 , respectively. It can be seen from Figure 6.6. that the location of vortex generators also has an influence on the flow field, and when $l=0.3$, the turbulent kinetic energy is minimum, while when $l=0.5$, compared with the traditional flapper, the impact is very small. Here is why: The flow separation point is at the intersection of plane and camber of the flapper, when $l=0.3$, vortex generators are in front of the separation point, the vortex generators can very good play, when $l=0.4$, vortex generators also ahead of the separation point, flow separation is also delayed, but the effect is a bit poor, when $l=0.5$, the tail of the vortex generators are near the separation point, the vortex generators are basically not functioning, as a result, the effect of delaying flow separation is the worst. If the vortex generator is too close to the nozzle, the jet flow of

the nozzle will be affected. The installation position of the vortex generator l should be relatively large, so $l=0.4$ is better.

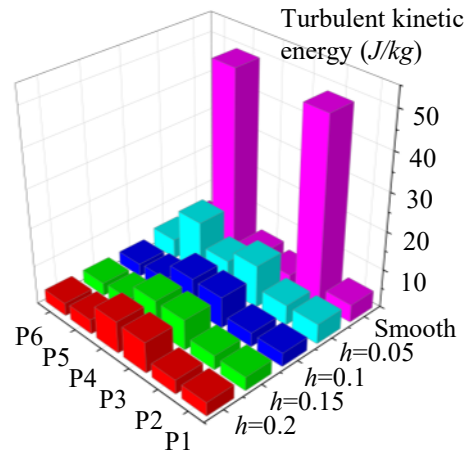


Figure 6.5. Turbulent kinetic energy of flow field corresponding to different vortex generator heights

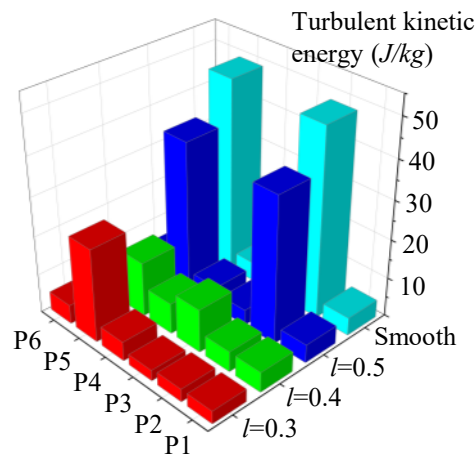


Figure 6.6. Turbulent kinetic energy of flow field corresponding to different vortex generator location

7. CONCLUSION

In this paper, a new flapper structure with vortex generators is proposed, which has the function of controlling the flow separation phenomenon of the pilot stage flow field and improve the stability of the flow field in flapper-nozzle pilot valve. The effectiveness of the vortex generators has been tested by CFD simulation method, and the conclusions can be summarized as follows.

The flow separation phenomenon exists in Flapper-nozzle pilot valve, and the greater the pressure is, the more obvious the flow separation phenomenon is.

Flow separation is delayed when the vortex generators are installed on the flapper. The larger the height of the vortex generator is, the more obvious the effect is. The vortex generator needs to be positioned in front of the separation point to function.

By controlling the flow of fluid, the vortex generators improve the stability of the flow field of pilot stage.

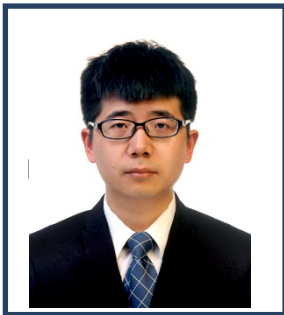
8. REFERENCES

- [1] Li S, Aung N, Zhang S, Cao J, Xue X. Experimental and numerical investigation of cavitation phenomenon in flapper–nozzle pilot stage of an electrohydraulic servo-valve. *Comput Fluids* 2013;88:590-8.
- [2] Washio S , Kikui S , Takahashi S . Nucleation and subsequent cavitation in a hydraulic oil poppet valve[J]. *ARCHIVE Proceedings of the Institution of Mechanical Engineers Part C Journal of Mechanical Engineering Science* 1989-1996 (vols 203-210), 2010, 224(4):947-958.
- [3] YaoWei Hu,JiangSheng Wang,JinJun Wang,Christian Breitsamter. Flow-structure interaction of an inverted flag in a water tunnel[J]. *Science China(Physics, Mechanics & Astronomy)*, 2019, 62(12):61-71.
- [4] Chen H , Chen B . Aerodynamic Performance Enhancement of Tiltrotor Aircraft Wings Using Double-Row Vortex Generators[J]. *International Journal of Aeronautical and Space Sciences*, 2021:1-11.
- [5] Tavernier D D , Ferreira C , A Viré, et al. Controlling dynamic stall using vortex generators on a wind turbine airfoil[J]. *Renewable Energy*, 2021(3).
- [6] Li L , Zhou B , H Huang, et al. Vortex generator design and numerical investigation for wake non-uniformity and cavitation fluctuation pressure reduction[J]. *Ocean Engineering*, 2021, 229:108965.
- [7] Che B , Chu N , Cao L. et al. Control effect of micro vortex generators on attached cavitation instability [J]. *Physics of Fluids*, 2019, 31(6): 064102.
- [8] Daniel B , Carlos F , De T D , et al. Experimental parameter study for passive vortex generators on a 30% thick airfoil[J]. *Wind Energy*, 2018, 21.
- [9] Baldacchino D , Manolesos M , Ferreira C , et al. Experimental benchmark and code validation for airfoils equipped with passive vortex generators[C]// *Journal of Physics: Conference Series*. 2016.
- [10] Xu Z , Hangan H . Scale, boundary and inlet condition effects on impinging jets[J]. *Journal of Wind Engineering & Industrial Aerodynamics*, 2008, 96(12):2383-2402.

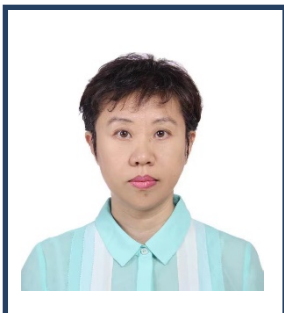
Biographies



Li Tong received the master's degree in mechanical engineering from Hunan University in 2017, He is currently studying for his doctorate at Harbin Institute of Technology with a research direction of servo valves.



Jinghui Peng received the master's degree and the philosophy of doctorate degree in mechatronics engineering from the Harbin Institute of Technology in 2011 and 2016, respectively. He is currently working as a Professor in the School of Energy Science and Engineering, Harbin Institute of Technology. His research areas include functional fluids, electrohydraulic servo-valve, fluid-structure interaction, vibration and noise suppression, and microfluidic microbial fuel cells.



Songjing Li received the Ph.D. from the Harbin Institute of Technology (HIT), China, in 1998. She is currently a Professor and the Head of the Department of Fluid Control and Automation, School of Mechanical Engineering, Harbin Institute of Technology. Her research topics include CFD for fluid power components and systems, microfluidic chips and systems, self-excited noise in hydraulic servo-valves and water generator from air.